05

Prospect of application of gradient cellular structures with controlled permittivity for 3D-printing of the Luneburg lens

© M.F. Akhmatnabiev,[1,2] M.V. Timoshenko,[2] M.M. Sychev,[1,2] A.A. Petrov,[3] S.V. Diachenko[1,2]

[1]Branch of B. P. Konstantinov Petersburg Nuclear Physics Institute of National Research Center „Kurchatov Institute“ — I.V. Grebenshchikov Institute of Silicate Chemistry,
199034, St. Petersburg, Russia
[2]St. Petersburg State Technological Institute (Technical University),
190013 St. Petersburg, Russia
[3]Scientific and Research Institute „Vector“,
197022 St. Petersburg, Russia
e-mail: svdiachenko@technolog.edu.ru

Received November 11, 2024
Revised February 24, 2025
Accepted February 27, 2025

The study included designing of a material for 3D-printing of the Luneburg lens and investigating electrical and mechanical properties of the cellular materials and controllability of their permittivity for use in manufacturing the lens. It is shown that by means of structures based on minimum-energy triply-periodic surfaces, it is possible to obtain the required values of permittivity by varying a degree of filling of space with matter. Geometries of the minimum-energy triply-periodic surfaces are selected, a formula of the dependence of permittivity on the degree of filling of the structure space is obtained, thereby making it possible to create intermediate layers of the Luneburg lens with a pre-defined value of permittivity.

Keywords: Luneberg lens, spherical lens, antenna lens, permittivity, additive technologies, 3D-printing, cellular materials, gradient materials, minimum-energy triply-periodic surfaces.

DOI: 10.61011/TP.2025.07.61453.417-24

Introduction

The VHG-range radio complexes (decimeter and centimeter waves) use various types of antennas. Of particular interest among them are spherical lenses made of dielectric materials, which are designed to form a required directional pattern (DP) in any direction and to scan space by means of it by moving an emitter or switching several emitters near its surface. The lenses are suitable for forming multi-beam directional patterns, which is important for many applications.

Taking into account the spherical symmetry of the lens, it is possible to simultaneously form several directional patterns of the antenna. At the same time, there is independence of formation of separate beams and high scanning performance under a condition of electrical switching [1].

In accordance with the classification given in the paper [2], the spherical lenses can be manufactured of a homogeneous and a inhomogeneous dielectric. However, in case of the homogeneous dielectric it is impossible to form a flat wave front on a lens aperture, which corresponds to the narrow directional pattern.

In VHF engineering, the most promising for application are the Luneburg lenses (LL) that are named after the German mathematician and physicist Rudolf Karl Luneburg and described by him in the paper [3]. He has shown in his study that the spherical lens refracts the beams arriving thereinto, so that they exit the lens towards a diameter crossing the source, if the refractive index $n(r)$ satisfies the condition (1):

$$n(r) = \sqrt{\varepsilon'(r)} = \sqrt{2 - \left(\frac{r}{R}\right)^2}, \qquad (1)$$

where n — the refractive index in the point r; $\varepsilon'(r)$ — relative permittivity of the lens material in the point r; r/R — a ratio of a current radial coordinate to the sphere radius.

In the classic Luneburg lens, this condition is realized by varying permittivity of the spherical lens from 2 in the center to 1 on the surface. The diagram of transmission of the beams is shown in Fig. 1.

A quite complicated technology of production of the multi-layer structures with the spherical symmetry is one of the main technological difficulties in manufacturing of the Luneburg lens-based antennas, which has for a long time restricted development of this field of antenna engineering.

In recent years, due to development of material science and improvement of the production technology, there is another surge of interest to the Luneburg lens.

In real conditions, it is difficult to accurately implement the required law of variation of the refractive index $n(r)$ in the Luneburg lens. Usually, the continuous dependence $\varepsilon(r)$ is replaced by a step dependence, as shown on Fig. 2. The number of the layers can vary, but it is seldom less than four or noticeably higher than ten.

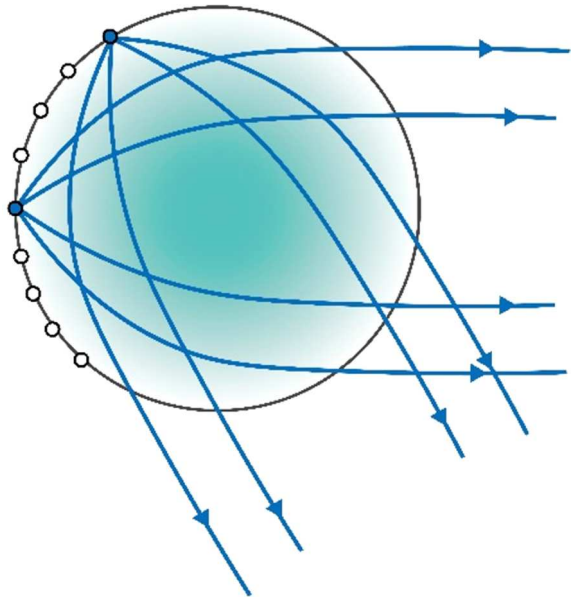

Figure 1. Diagram of transmission of the beams in the spherical Luneburg lens.

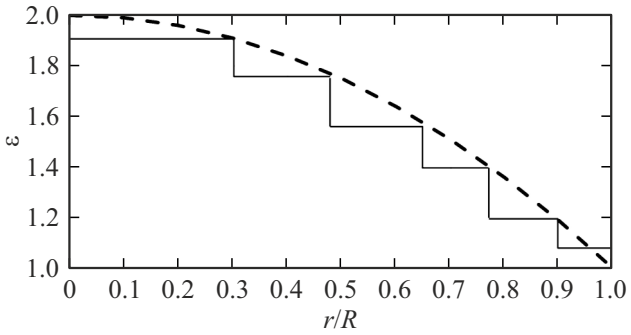

Figure 2. Exemplified dependence of permittivity ε in the Luneburg lens on the value of r/R; the dashed line — as per the equation (1), the solid line — when manufacturing the Luneburg lens by layers of different permittivity.

Traditionally, the Luneburg lenses have been assembled from spherical layers that differ in permittivity, wherein its manufacturing is labor-consuming. Besides, in doing so, there is no smooth variation of permittivity. Application of fillers with high values — when manufacturing the materials it complicates the technology and does not result in drastic reduction of the average density of the lens. Presently, due to introduction of metamaterials, there is widespread use of the Luneburg lenses produced by „MatSing“ [4] in accordance with their developed technology. However, these structures have a low strength and permittivity varies discretely.

Various methods are used to adjust the value of permittivity. The most widely used method of manufacturing this lens is to divide the sphere volume into layers of a homogeneous material (ball layers), whose permittivity increases from the external radius of the sphere to the center. Since the layers have a complex hemisphere shape, the most promising method of manufacturing at the moment is 3D-printing.

In order to obtain various values of permittivity in these layers, different methods are used. In general, they are reduced to variation of a printing density. For example, by varying a size of the elementary cubic cell [5,6] or by varying a diameter of the cylindrical cell [7]. Besides, there are other methods of creating the Luneburg lens with variable permittivity: varying a thickness of the dielectric plate in the waveguide [8–10], drilling holes in the dielectric plate to control effective permittivity by the density of the holes [11–13], varying permittivity by means of additional metamaterials [14].

The present study proposes a new approach to developing the Luneburg lens, which consists in using the gradient cellular materials based on the triply periodic minimal surfaces (TPMS) with controlled permittivity, which are manufactured by means of additive technologies.

The TPMS are a class of analytically pre-defined surfaces that have three-dimensional periodicity and a zero average curvature and consist of recurring elements with the least possible area. The application interest to these surfaces has quite recently appeared, as the materials with the TPMS geometry can be manufactured only using the additive technologies. Owing to its smooth saddle-like shape, the structures with the TPMS geometry demonstrate no stress concentration, thereby positively affecting their mechanical characteristics and a value of energy absorption [15–21]. Besides, using the TPMSes, it is possible to created the gradient structures [22] by varying the thickness of the cell wall, thereby adjusting material porosity and respectively controlling permittivity in the required directions.

Thus, a design of the spherical Luneburg lens of the TPMS-based gradient structures will allow improving the physical-mechanical indicators as well as smoothly varying permittivity inside the Luneburg lens, approaching the law of variation of permittivity in the sphere as obtained by Luneburg.

The aim of the present study is to apply the cellular dielectric structures with the TPMS geometry, which are obtained using the additive technologies, in creation of the Luneburg lens. Using 3D-printing and TPMS, it is possible to manufacture the gradient structures with variation of their porosity, thereby continuously varying permittivity along the sphere radius, as much as possible approaching the law of variation of the permittivity coefficient in the spherical body as deduced by Luneburg.

1. Materials and methods

Since the TPMSes can be manufactured only by means of the additive technologies, a technology of obtaining a highly-filled composite (filled with a dielectric) was developed for 3D-printing in Fused Deposition Modeling (FDM) [23].

The main raw material was ABS 2332 (ABS) — acrylonitrile butadiene styrene (a thermoplastic amorphous triple copolymer of acrylonitrile, butadiene and styrene) produced by PJSC „SiBUR Holding“ and rutile titanium dioxide (TiO_2) produced by „Crimea TITAN“ under the grade „Crimea TiOx220“ (TU 2321-001-17547702-2014), with the particle size of 15 μm. Selection of ABS as a printing material was based on the fact that it is one of most widely-used materials in the sphere of the additive technologies and it has a high value of permittivity (at 10 GHz: $\varepsilon = 2.6$) and relatively high strength characteristics (the bending strength $\sigma_i = 69$ MPa, the tensile strength $\sigma_s = 45$ MPa).

For the filler, titanium dioxide (TiO_2) was used and it has high dielectric properties at the standard temperature conditions ($\varepsilon = 15 - 170$, $\mathrm{tg}\,\delta = 0.0016$ a the frequency of 1 MHz) [24,25], which is extremely important when using the lens. It is known that filling the polymer with titanium dioxide can make it possible to significantly increase permittivity of the polymer [26] and, therefore, it is possible to produce the structure with high porosity and required permittivity. The present study has the samples of the ABS material manufactured, which have a various degree of titanium dioxide filling χ, mass %: 0, 20, 40. The maximum percent of titanium dioxide filling was 40 %, as a filament made of the material with the high content of titanium dioxide was spontaneously destroyed, thereby making it impossible to print by it.

For the designed composite materials, technological parameters of 3D-printing were selected. It was printed by Fused Deposition Modeling in the 3D-printer „Artillery Sidewinder X1“ with a nozzle diameter of 0.4 mm at the extruder temperature of 240 °C and the table temperature of 90 °C with a printing rate of 60 mm/s.

In order to study permittivity of the composite, experimental samples of the designed composites were printed with 100 % filling during printing. The samples for measuring permittivity were rectangular parallelepipeds with the sizes 23 × 10 × 10 mm.

The permittivity was measured in a waveguide path in JSC „Scientific and Research Institute Vector“ by completely filling a cross section of the short-circuited waveguide [27]. A measurement line R1-28 was used during the measurements. As a result of measurements, permittivity of the printed solid samples (the sample filling degree $\varphi = 100\,\%$) of the produced filled composite at 10 GHz was $\varepsilon(\mathrm{ABS} + 40\,\%\mathrm{TiO_2}) = 3.95$, and permittivity of the unfilled ABS plastic was $\varepsilon(\mathrm{ABS}) = 2.6$.

The geometry of the structures was based on the triply periodic minimal surfaces that have relatively high mechanical properties among the cellular materials [28]. It is known that these structures can be obtained only by 3D-printing. When using the additive technologies, it is possible to manufacture the TPMS-based structures with anisotropy of the properties, thereby implementing continuous variation of permittivity by gradient variation of porosity (the space filling degree, respectively). That is why, for designing the gradient structures, the experiments included selection of the most reproducible TPMS geometries without hanging structural elements that result in formation of defects.

The 5 TPMS geometries were selected and modeled in the „MS Lattice“ software (Fig. 3), and then printed in the 3D-printer. The samples were parallelepipeds of the size 23 × 10 × 10 mm. The selected TPMSes were printed from the ABS plastic with the various content of TiO_2. At this, it varied the space filling degree to obtain various degrees of ε. Then, measurements of their permittivity were performed on a series of the three samples, wherein the measurement error was about 3 %. The experimental data were analyzed by the „Origin“ software; in particular, the magnitude k of the equation (2) was determined based on a plotted curve with the largest coefficient of determination.

For long-term operation of the Luneburg lens, its manufacturing requires structures with high strength indicators. In order to determine the TPMS geometry with the best mechanical properties, physical-mechanical tests of the samples made of the ABS material with the various degree of titanium dioxide filling χ were performed. The compression tests samples were cubes with a facet size of 30 mm with the various TPMS geometry. The tests were performed in accordance with [29]. The samples for bending tests were manufactured as beams (the sample size 80 × 10 × 4 mm), while the samples for tensile tests were manufactured as blades (the sample of the 1A type) with 100 % filling. The samples were sized in accordance with regulatory documents [30,31]. The tests were performed in a table-top universal tester „Metrotrest REM-50-A-1-1“ at the loading rate of 5 mm/min.

Specific strength indicators were obtained by assigning the result of the mechanical tests to the sample density. The sample weight was measured on the analytical scales „Ohaus Pioneer PA−214C“. The beam volume was measured geometrically by overall dimensions using the vernier caliper „ShTsTs-1-150-0,01“; the blade volume was calculated in the 3D-model by the „SolidWorks“ software.

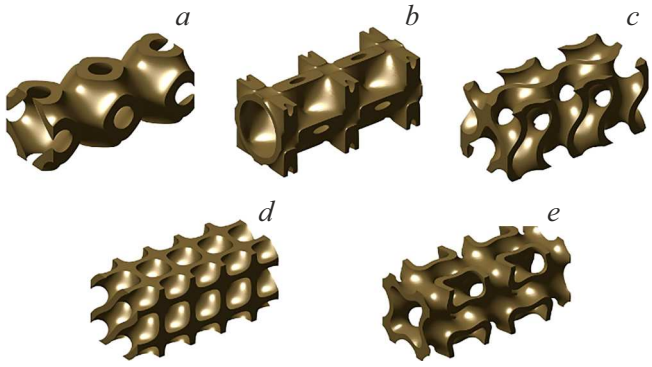

Figure 3. Types of the TPMS geometries selected for printing: „Primitive“ (*a*), „IWP“ (*b*). „Gyroid“ (*c*), „Diamond“ (*d*), „Neovius“ (*e*).

2. Results

The experiments included selection of the most reproducible TPMS geometries. As a result of printing of the selected samples, it was concluded that the least quantity of visible defects was observed in the following kinds: „Gyroid“, „Diamond“, „Neovius“ (Fig. 4).

Fig. 5 shows the dependence between a percent of space filling and permittivity of the printed samples with the various TPMS geometry. The obtained dependence is described by the Lihteneker formula for the composite materials (2), in which the coefficient k was selected by variation [32]. Owing to the obtained dependence, it is possible to predict the properties of the Luneburg lens intermediate layers:

$$\varepsilon^k = \varphi \cdot \varepsilon_1^k + (1 - \varphi) \cdot \varepsilon_2^k, \qquad (2)$$

where ε_1 — the permittivity of the medium 1 (the material), ε_2 — the permittivity of the medium 2 (air), φ — the degree of space polymer filling, $k = 0.45694$ — the coefficient depending on the system isotropy.

The form of the experimental curves $\varepsilon = f(\varphi)$ of Fig. 5 can be described by a quadratic dependence

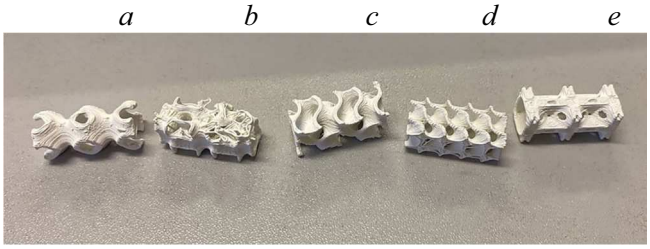

Figure 4. Printed samples of the various geometries: „Primitive“ (*a*), „IWP“ (*b*), „Gyroid“ (*c*), „Diamond“ (*d*), „Neovius“ (*e*).

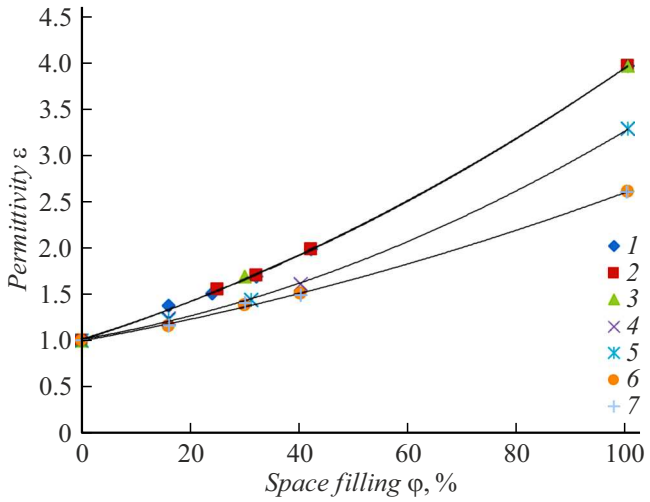

Figure 5. Dependence of permittivity ε on the degree of space filling φ. *1* — Gyroid ($\chi = 40\,\%$), *2* — Diamond ($\chi = 40\,\%$), *3* — Neovius ($\chi = 40\,\%$), *4* — Gyroid ($\chi = 20\,\%$), *5* — Diamond ($\chi = 20\,\%$), *6* — Gyroid ($\chi = 0\,\%$), *7* — Diamond ($\chi = 0\,\%$).

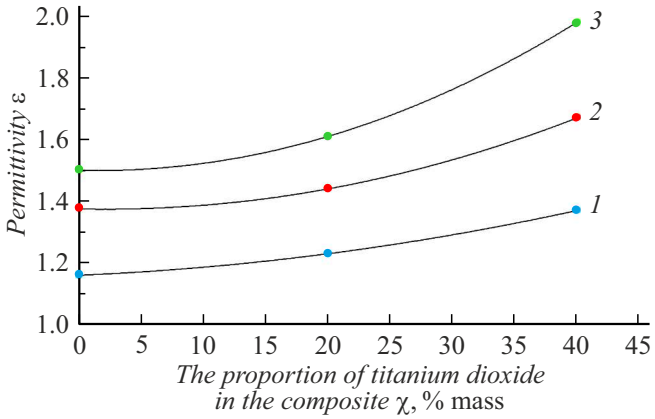

Figure 6. Dependence of permittivity ε on titanium dioxide filling χ: *1* — $\varphi = 15\,\%$; *2* — $\varphi = 30\,\%$; *3* — $\varphi = 40\,\%$.

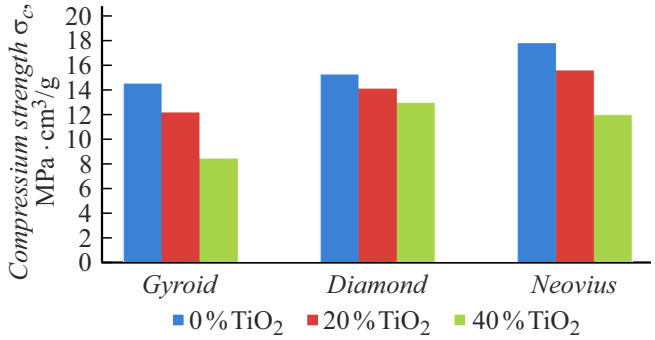

Figure 7. Results of mechanical compression tests of TPMSes.

$(a\varphi^2 + b\varphi + c = \varepsilon)$, and using it, it is possible to determine the required values of the filling degree for the required value of permittivity. In particular, for the curves *1–3* when $\varepsilon = 1.1$ (at the lens edge) the filling degree takes the value $\varphi_1 = 5.1\,\%$, and when $\varepsilon = 2$ (in the lens center) does it $\varphi_2 = 43.3\,\%$. The obtained values of φ can be used for designing the device made of the material with a titanium dioxide proportion $\chi = 40\,\%$.

Fig. 6 shows the dependence of the value of permittivity of the TPMS samples on the quantity of titanium dioxide in the composite.

Based on the results of the mechanical tests, determined are the compression strength of the TPMSes (Fig. 7), the tensile strength and the bending strength (see Table) thereof and their specific values.

3. Discussion of the results

Among the printed TPMS samples, the most successful in terms of the printing quality are the samples „Gyroid“, „Diamond“ and „Neovius“. The printed samples „Primitive“, „IWP“ exhibited significant defects. Probably, it is related to presence of the hanging structural elements that are difficult to be reproduced when printing the small-size

Results of the mechanical tests of the 3D-printed solid witness samples with various titanium dioxide filling

Strength σ	Filling degree χ		
	0 %	20 %	40 %
σ_t, MPa	29.8	27.1	26.5
$\sigma_{t.s}$, MPa·cm^3/g	32.8	25.2	19.5
σ_f, MPa	48.7	47.3	44.1
$\sigma_{f.s.}$, MPa·cm^3/g	53.3	44.0	34.0

Note. (σ_t) — the tensile strength; $(\sigma_{t.s})$ — the specific tensile strength; (σ_f) – the bending strength; $(\sigma_{f.s})$ — the specific bending strength.

samples, as well as to the fact that the used filament has a nonuniform diameter along its length due to presence of the filler. Thus, the mentioned geometries were excluded from further consideration.

It follows from the results of measurement of permittivity (Fig. 5) that with decrease of the degree of space filling φ, the value ε decreases, which is related to increase of the size of air-filled pores. Besides, based on the obtained results, it follows that varying the filling degree resulted in production of the material with the value of ε equal to 2 — the sample with the geometry „Diamond“ and „Gyroid“ with the content of TiO_2 $\chi = 40\,\%$ and the filling degree $\varphi = 42\,\%$.

The minimum obtained permittivity $\varepsilon = 1.16$ is quite close to the required value and can be used in the layers that are close to the Luneburg lens surface. This value of permittivity was obtained in the sample with the geometry „Gyroid“ and „Diamond“ when $\varphi = 16\,\%$. It should be noted that the TPMS geometry insignificantly affects the value of permittivity, as with almost the same filling the value of permittivity of all the structures was the same (Fig. 5, the curves *1–3*). At the same time, there is an observed exponential function between the percent of space filling φ and permittivity ε in accordance with (2), thereby making it possible to predict values of permittivity of the Luneburg lens layers.

Based on the study results, the most promising in terms of practical application were the geometries „Diamond“ and „Gyroid“. These TPMSes were printed with the least visible defects and the value of permittivity can be varied in the wide range. No small value of permittivity could be obtained in the geometry „Neovius“ since with small fillings the structure was not reproduced, so it was decided to abandon further use of this TPMS.

With increase of the quantity of titanium dioxide in the composite, the value of permittivity is growing as expected (Fig. 6). At the same time, there is an observed quadratic dependence of ε on the quantity of titanium dioxide, which is most pronounced in the samples with large space filling.

Based on the obtained data for the mechanical characteristics (Fig. 7), it follows that the largest compression strength was demonstrated by the samples with the geometry „Neovius“, while the least value thereof was observed for the samples with the geometry „Gyroid“. The samples of all the geometries exhibit the same dependence of the strength on the degree of titanium dioxide filling: with increase of the content of titanium dioxide the specific value of the strength decreases. At this, the structures with the large percent of TiO_2 filling to a greater degree exhibit brittle fracture (after the test partial fracture of the sample was recorded), while the samples made of the unfilled plastic exhibit only plastic strain without formation of visible cracks. This behavior of the material may be attributed to the fact that with the large quantity of the filler there are more phase interfaces formed in the structure, which result in increase of the stress concentration and formation of a large number of microcracks. The unfilled ABS contains no titanium dioxide particle and the behavior of the material under compression loading is typical the plastic materials. It also follows from Fig. 7 that with filling the plastic with titanium dioxide $\chi = 40\,\%$ the value of the specific strengths turns out to be the largest for the geometry „Diamond“, whence it can be deduced that printing of this geometry with the large quantity of the filler turns out to be with the least defects.

The specific strength indicators for rupture and bending also decrease with addition of titanium dioxide (see Table). It can be attributed to the fact that due to increase of the filler content there is observed adhesion interaction between the polymer and the filler, which is substantially less than the polymer strength [33]. At this, the cracks formed in the composite under mechanical loading probably proliferate along a polymer-filler boundary. With increase of the quantity of the filler in the composite the titanium dioxide particles form agglomerates, thereby contributing to reduction of adhesion and facilitating crackability at the interphase boundaries.

Conclusion

The study included designing of the composite material that is a polymer matrix based on the ABS plastic and filled with titanium dioxide. It is shown that with increase of the percent of the filler permittivity increases. By using this material in the 3D-printing, it is possible to vary permittivity within the range from 1.16 to 2 that is required for creation of the Luneburg lens.

Based on the designed polymer material, using the FDM technology, the various TPMS types are manufactured: „Primitive“, „IWP“, „Gyroid“, „Diamond“, „Neovius“. In accordance with selection criteria: the printing quality, reproducibility, the mechanical properties, provision of the required range of permittivity, the weight, etc. the two most suitable TPMS geometries are selected: „Gyroid“ and „Diamond“. For the samples of the selected geometries, the dependence of permittivity on the degree of space filling has been determined. Using this dependence, it is possible to obtain the Luneburg lens intermediate layers

with certain values of ε. As a result, for both the samples the values of ε are obtained in the required range. However, for the geometry „Diamond“ the greater values of the compression strength for TPMS are obtained: $\sigma_c = 15.23$ (when $\chi = 0\,\%$), 14.09 (when $\chi = 20\,\%$), 12.92 MPa (when $\chi = 40\,\%$). It should be noted that it is still possible to use the structure „Gyroid“ in the future when designing the Luneburg lens due to its lesser weight with other geometrical parameters being the same.

The main conclusions:

1) the geometry of the cellular structure is determined for manufacturing the spherical Luneburg lens of the designed composite material — „Diamond“;

2) for the designed material, there is the exhibited exponential function of permittivity ε on the degree of space filling φ ($\varepsilon \sim \varphi^2$) and the titanium dioxide proportion χ ($\varepsilon \sim \chi^2$);

3) for the designed material, the value of permittivity at the same degree of space filling is still the same for the various TPMS geometries;

4) it is proven that it is possible to apply the gradient cellular structures for designing the antenna devices, which have the required values of permittivity of the material ($\varepsilon = 1.16 - 2$).

Practical importance. Application of the gradient cellular structures will make it possible to obtain continuous variation of permittivity along the radius in the spherical Luneburg lens.

Further research will be dedicated to designing a spherical Luneburg lens prototype based on TPMS with gradient variation of the properties, thereby improving its electrical characteristics in radiolocation with a wide space scanning angle, as well as its mechanical characteristics for its application in severe climatic conditions and under external impacts in aviation and sea vessels.

Funding

This study was supported by a grant from the Russian Science Foundation (project No. 20-73-10171).

Conflict of interest

The authors declare that they have no conflict of interest.

References

[1] B.A. Panchenko. Antenny, **12** (2010) (in Russian).
[2] E.G. Zelkin, R.A. Petrova. *Linzovye antenny* (Sovetskoe radio, M., 1974) (in Russian).
[3] R.K. Luneburg. *Providence*, RT (Brown Univ. Press, 1944)
[4] *Sphere Antennas.* Electronic source. Available at: www.matsing.com URL: https://www.matsing.com/product-category/antennas/product-families/sphere-antennas/ (date of access: 19.02.2025)
[5] M. Liang, W. Ng, K. Chang, K. Gbele, M.E. Gehm, H. Xin. IEEE Transactions on Antennas and Propagation, **62** (4), (2014). DOI: 10.1109/TAP.2013.2297165
[6] R.A. Bahr, A.O. Adeyeye, S. Van Rijs, M.M. Tentzeris. *3D-Printed Omnidirectional Luneburg Lens Retroreflectors for Low-Cost mm-Wave Positioning, 2020 IEEE International Conference on RFID (RFID)* (Orlando, FL, USA, 2020), p. 1-7. DOI: 10.1109/RFID49298.2020.9244891
[7] K. Liu, C. Zhao, S. Qu, Y. Chen, J. Hu, S. Yang. IEEE Antennas and Wireless Propagation Lett., **20** (3), (2021). DOI: 10.1109/LAWP.2021.3054042
[8] G. Peeler, D. Archer. IRE Trans. Antennas Propag., **1** (1), (1953).
[9] X. Wu, J. Laurin. IEEE Trans. Antennas Propag., **55** (8), (2007). DOI: 10.1109/TAP.2007.901843
[10] L. Xue, V. Fusco. IET Microw Antennas Propag., **2** (2), (2008). DOI: 10.1049/IET-MAP%3A20070146
[11] L. Xue, V.F. Fusco. IET Microw. Antennas Propag., **1** (3), (2007). DOI: 10.1049/iet-map:20050203
[12] K. Sato, H. Ujiie. Electro. Commun. Jpn., **85** (9), (2002). DOI: 10.1002/ecja.1120
[13] C.S. Lee, S.W. Lee, R. Davis, J. Tsui Microw. Opt. Technol. Lett., **5** (2), (1992).
[14] Q. Cheng, H.F. Ma, T.J. Cui. Appl. Phys. Lett., **95** (18), (2009). DOI: 10.1063/1.3257375
[15] J. Feng, J. Fu, X. Yao, He Yong. Intern. J. Extreme Manufactur., **4** (2), (2022). DOI: 10.1088/2631-7990/ac5be6
[16] V. Shevchenko, S. Balabanov, M. Sychov, L. Karimova. ACS Omega, **8** (30), (2023). DOI: 10.1021/acsomega.3c01631
[17] S.V. Balabanov, A.I. Makogon, M.M. Sychev, A.A. Evstratov, A. Regazzi, J.M. Lopez-Cuesta. Tech. Phys., **65** (2), 211 (2020). DOI: 10.1134/S1063784220020036
[18] M.M. Sychov, L.A. Lebedev, S.V. Dyachenko, L.A. Nefedova. Acta Astronautica, **150**, (2018). DOI: 10.1016/j.actaastro.2017.12.034
[19] S.V. Diachenko, L.A. Lebedev, M.M. Sychov, L.A. Nefedova. Tech. Phys., **63** (7), (2018). DOI: 10.1134/S1063784218070101
[20] X. Fan, Q. Tang, Q. Feng. Intern. J. Mechan. Sci., **204**, (2021). DOI: 10.1016/j.ijmecsci.2021.106586
[21] X. Zhang, L. Jianga, X. Yanb. Virtual Phys. Prototyping., **18** (1), (2022). DOI: 10.1080/17452759.2022.2120406
[22] S. Yu, J. Sun, J. Ba. Mater. Design, **182**, (2019). DOI: 10.1016/j.matdes.2019.108021
[23] M.V. Timoshenko, S.V. Balabanov, M.M. Sychov. Glass Phys. Chem., **49**, (2023). DOI: 10.31857/S0132665123600243
[24] P. Veselý, D. Froš, T. Hudec, J. Sedláček, P. Ctibor, K. Dušek. Virtual Phys. Prototyping., **18** (1), (2023). DOI: 10.1080/17452759.2023.2170253
[25] D.W. Richerson, W.E. Lee. *Modern Ceramic Engineering: Properties, Processing and Use in Design* (CRC Press, 2018)
[26] M.A. Ramazanov, F.V. Hajiyeva, A.M. Maharramov. Integrated Ferroelectrics, **192** (1), (2018). DOI: 10.1080/10584587.2018.1521658
[27] A.A. Brandt, *Issledovanie dielektrikov na sverkhvysokikh chastotakh* (Fizmatgiz, M., 1963) (in Russian).
[28] M.P. Desole, A. Gisario. Intern. J. Adv. Manufacturing Technol., **132** (3−4), (2024). DOI: 10.1007/s00170-024-13430-0
[29] *Plastmassy. Metod ispytaniya na szhatie* (GOST 4651−2014, Standartinform, M., 2014), 26 s. (in Russian).
[30] *Plastmassy. Metod ispytaniya na rastyazhenie* (GOST 11262−2017, Standartinform, M., 2017), 24 s. (in Russian).

[31] *Plastmassy. Metod ispytaniya na staticheskii izgib* (GOST 4648−2014, Standartinform, M., 2014), 25 s. (in Russian)
[32] M.M. Sychev, T.S. Minakova, Yu.G. Slizhov, O.A. Shilova. *Kislotno-osnovnye kharakteristiki poverkhnosti tverdykh tel i upravlenie svoistvami materialov i kompozitov* (Khimizdat, SPb., 2022) (in Russian).
[33] I. Ozsoy, A. Demirkol, A. Mimaroglu, H. Unal, Z. Demir. J. Mechan. Eng., **61** (10), (2015). DOI: 10.5545/sv-jme.2015.2632

Translated by M.Shevelev